ADVANCED MATERIALS
www.advmat.de

Achieving Fast Charge Separation and Low Nonradiative Recombination Loss by Rational Fluorination for High-Efficiency Polymer Solar Cells

Chenkai Sun, Fei Pan, Shanshan Chen, Rui Wang, Rui Sun, Ziya Shang, Beibei Qiu, Jie Min, Menglan Lv,* Lei Meng,* Chunfeng Zhang, Min Xiao, Changduk Yang, and Yongfang Li**

Four low-cost copolymer donors of poly(thiophene-quinoxaline) (PTQ) derivatives are demonstrated with different fluorine substitution forms to investigate the effect of fluorination forms on charge separation and voltage loss (V_{loss}) of the polymer solar cells (PSCs) with the PTQ derivatives as donor and a A–DA'D–A-structured molecule Y6 as acceptor. The four PTQ derivatives are PTQ7 without fluorination, PTQ8 with bifluorine substituents on its thiophene D-unit, PTQ9, and PTQ10 with monofluorine and bifluorine substituents on their quinoxaline A-unit respectively. The PTQ8- based PSC demonstrates a low power conversion efficiency (PCE) of 0.90% due to the mismatch in the highest occupied molecular orbital (HOMO) energy levels alignment between the donor and acceptor. In contrast, the devices based on PTQ9 and PTQ10 show enhanced charge-separation behavior and gradually reduced V_{loss}, due to the gradually reduced nonradiative recombination loss in comparison with the PTQ7-based device. As a result, the PTQ10-based PSC demonstrates an impressive PCE of 16.21% with high open-circuit voltage and large short-circuit current density simultaneously, and its V_{loss} is reduced to 0.549 V. The results indicate that rational fluorination of the polymer donors is a feasible method to achieve fast charge separation and low V_{loss} simultaneously in the PSCs.

Polymer solar cells (PSCs) are promising solar energy conversion technology because of their characteristic of simple device structure, light weight, flexibility, and low-cost fabrication by solution processing.[1,2] Due to the significant innovations in efficient photovoltaic materials,[3–11] interface buffer layer materials,[12–16] and device engineering,[17–19] PSCs have achieved great progress in the past few years, and the power conversion efficiency (PCE) of the PSCs has increased to over 15%.[11,20,21] Nevertheless, PCE of the PSCs still lags behind the inorganic and perovskite solar cells (pero-SCs), which is mainly due to the higher voltage loss (V_{loss}) from the optical bandgap (E_g) of the photoactive layer materials to the open-circuit voltage (V_{oc}) of the devices.[22] Normally, the V_{loss} in the champion crystal silicon (*c*-Si) solar cells and pero-SCs are 0.4–0.55 V, and it can be reduced to amazing 0.3 V in GaAs solar cells. In contrast, V_{loss} of the highly efficient PSCs are around 0.6 V or higher.[23–25]

C. Sun, F. Pan, Z. Shang, B. Qiu, Dr. L. Meng, Prof. Y. Li
Beijing National Laboratory for Molecular Sciences
CAS Key Laboratory of Organic Solids
Institute of Chemistry
Chinese Academy of Sciences
Beijing 100190, China
E-mail: menglei@iccas.ac.cn; liyf@iccas.ac.cn

C. Sun, F. Pan, Z. Shang, B. Qiu, Prof. Y. Li
School of Chemical Science
University of Chinese Academy of Sciences
Beijing 100049, China

Dr. S. Chen
MOE Key Laboratory of Low-Grade Energy Utilization Technologies and Systems
CQU-NUS Renewable Energy Materials & Devices Joint Laboratory
School of Energy & Power Engineering
Chongqing University
Chongqing 400044, China

The ORCID identification number(s) for the author(s) of this article can be found under https://doi.org/10.1002/adma.201905480.

DOI: 10.1002/adma.201905480

Dr. S. Chen, Prof. C. Yang
Department of Energy Engineering
School of Energy and Chemical Engineering
Low Dimensional Carbon Materials Center
Ulsan National Institute of Science and Technology (UNIST)
Ulsan 689-798, Republic of Korea

Dr. R. Wang, Prof. C. Zhang, Prof. M. Xiao
National Laboratory of Solid State Microstructures
School of Physics, and Collaborative Innovation Center of Advanced Microstructures
Nanjing University
Nanjing 210093, China

R. Sun, Prof. J. Min
The Institute for Advanced Studies
Wuhan University
Wuhan 430072, China
E-mail: min.jie@whu.edu.cn

Prof. M. Lv
School of Chemical Engineering
Guizhou Institute of Technology
Guiyang 550003, China
E-mail: lvmenglan@git.edu.cn

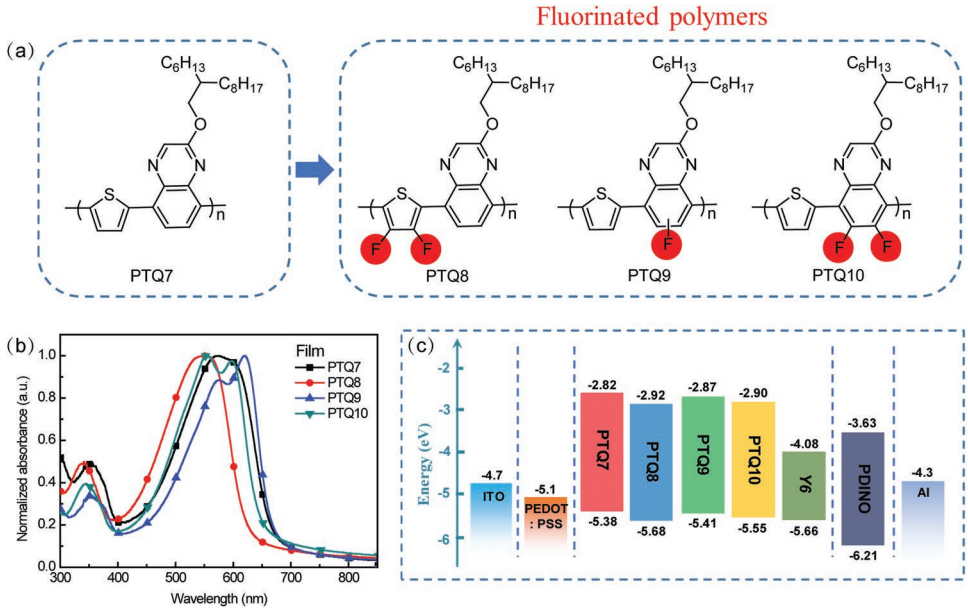

Figure 1. a) Molecular structures and b) the normalized absorption spectra of the polymers PTQ7, PTQ8, PTQ9, and PTQ10. c) Energy level diagram of the related materials used in the PSCs.

The higher V_{loss} of PSCs are due to two issues: radiative recombination loss and nonradiative recombination loss.[22,26] For an ideal PSC based on Shockley–Queisser (SQ) limit, a theoretical maximum V_{oc} can be obtained if the unescapable radiative recombination loss generating from the absorption above the optical bandgap is the only contribution part of V_{loss}.[27] Nevertheless, in a realistic PSC device, the additional radiative recombination loss, which is due to a nonabrupt absorption onset and the presence of subgap charge-transfer, (CT) state can further increase the V_{loss}; thus, the energy offset ($E_g - E_{CT}$) between E_g and CT state should be minimized to reduce the V_{loss} from this part.[28] Actually, this energy offset is commonly considered to be the driving force for charge separation, and it is believed that sufficient driving force is necessary to achieve efficient and fast charge separation thus large photogenerated current in the devices. Consequently, it seems that getting both high V_{oc} and large short-circuit current density (J_{sc}) was restricted in the PSCs. On the other hand, significant nonradiative recombination loss because of the extremely low-electroluminescence (EL) quantum efficiency (EQE_{EL}) in PSCs cannot be neglected, and it actually contributes to the main losses part of the V_{loss}. Therefore, achieving fast charge separation under small driving force and suppressing nonradiative recombination are crucial for obtaining the high-efficiency PSCs.

There have been several works to study the charge-separation behavior and V_{loss} of the PSCs according to the optimized molecular structures,[21] selected donor–acceptor (D–A) pairs,[29] and device engineering.[30] Here, we demonstrate four low-cost D–A copolymer donors[31,32] of poly(thiophene–quinoxaline) (PTQ) derivatives with different fluorine substitution: PTQ7 without fluorination, PTQ8 with two fluorine substituents on its thiophene D-unit, PTQ9 and PTQ10[7] with one or two fluorine substituents on their quinoxaline (Qx) A-unit, respectively, for investigating the effect of fluorination forms of the PTQ derivatives on charge-separation behavior and nonradiative recombination loss of the PSCs with the PTQ derivatives as donors and a narrow bandgap n-type organic semiconductor (n-OS) Y6[11] as acceptors. Molecular structures of the four PTQ derivatives are shown in **Figure 1**a. PTQ8 shows a drastically downshifted highest occupied molecular orbital (HOMO) energy level, which leads to a high V_{oc} of 0.89 V, but its device demonstrates a poor PCE of 0.90% with a low J_{sc} and low fill factor (FF) because of the extremely poor charge separation and transportation in the blend resulting from the negative HOMO energy level offset between PTQ8 and Y6. While PTQ9 and PTQ10 exhibit moderately downshifted HOMO energy levels matching with the energy level of acceptor Y6. The PTQ9-based and PTQ10-based devices show gradually enhanced charge-separation and -transport behavior when increasing the number of F atoms on their Qx A-unit from the light intensity measurements and the transient absorption (TA) spectra. Moreover, the PSCs based on PTQ9 and PTQ10 as donors show gradually increased V_{oc} of 0.82 and 0.87 V with gradually reduced V_{loss} of 0.602 and 0.549 V due to the gradually reduced nonradiative recombination loss of 0.25 and 0.23 eV in comparison with the device based on PTQ7 (0.35 eV) without fluorination, respectively. As a result, the PTQ10-based device demonstrates an impressive PCE of 16.21% with a high V_{oc} of 0.87 V and a large J_{sc} of 24.81 mA cm^{-2}, and it is worth noting that the nonradiative recombination loss of 0.23 eV and V_{loss} of 0.549 V are one of the lowest nonradiative recombination loss values and V_{loss} values of the high-efficiency PSCs, respectively. The results indicate that rational fluorination of the polymer donors is the feasible method to achieve fast charge separation and low nonradiative

Prof. Y. Li
Laboratory of Advanced Optoelectronic Materials
College of Chemistry
Chemical Engineering and Materials Science
Soochow University
Suzhou, Jiangsu 215123, China

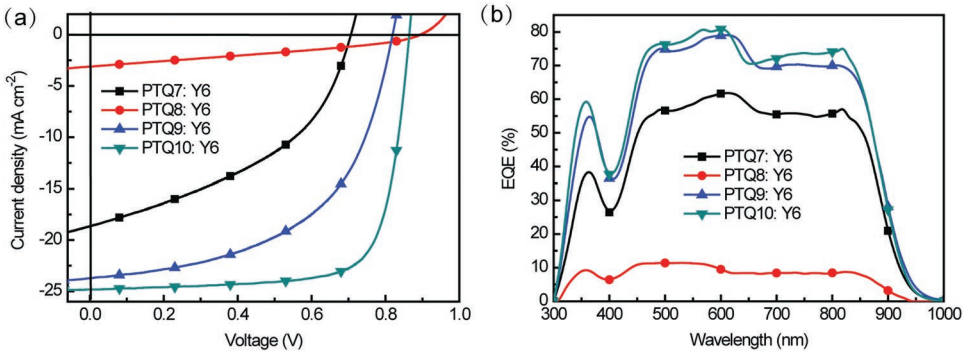

Figure 2. a) *J–V* curves of the PSCs based on polymer:Y6, under the illumination of AM 1.5G, 100 mW cm^{-2}. b) EQE spectra of the corresponding PSCs based on polymer:Y6.

recombination loss in the PSCs, which is beneficial for obtaining the highly efficient PSCs with both high V_{oc} and large J_{sc}.

The detailed synthesis procedures of the four PTQ derivatives are described in the Supporting Information. The number-average molecular weights (M_n) of the polymers PTQ7, PTQ8, PTQ9, and PTQ10 are measured to be 19.6, 20.8, 25.1, and 30.2 kDa with corresponding polydispersity index (PDI) values of 2.3, 1.6, 2.0, and 1.6 by high-temperature gel permeation chromatography (GPC), respectively (Table S1, Supporting Information).

Figure 1b shows the normalized UV–vis absorption spectra of the four polymers in films, and the corresponding optical data are shown in Table S1 (Supporting Information). All the four polymers display strong absorption from 450 to 600 nm with the optical bandgaps of 1.87, 2.00, 1.87, and 1.92 eV for the polymers PTQ7, PTQ8, PTQ9, and PTQ10, respectively. Compared to the single absorption peak of polymers PTQ7 and PTQ8, polymers PTQ9 and PTQ10 show well-defined absorption profiles with vibronic shoulders in the longer-wavelength range, which indicates the existence of ordered aggregation and strong π–π stacking interaction in their thin films. The cyclic voltammetry (CV) measurements are employed to evaluate the electronic energy levels of the four polymers, as shown in Figure S1 (Supporting Information), and their E_{HOMO}/E_{LUMO} were measured to be –5.38/–2. 82, –5.68/–2.92, –5.41/–2.87, and –5.55/–2.90 eV from their onset oxidation and onset reduction potentials, respectively (Figure 1c). As expected, the polymer PTQ8 has the deepest HOMO energy level due to the double-substituted F atoms on its thiophene D-unit, and the polymers PTQ9 and PTQ10 show gradually downshifted HOMO energy levels in comparison with PTQ7 due to the gradually increased number of F atoms on the Qx A-unit.

Photovoltaic properties of the four PTQ derivative donors were studied by fabricating the traditional structured PSCs with the device structure of indium tin oxide (ITO)/poly(3,4-ethylenedioxythiophene):poly(styrene-sulfonate) (PEDOT:PSS)/polymer:Y6/perylenediimide functionalized with amino N-oxide (PDINO)/Al. **Figure 2**a shows the current density–voltage (*J–V*) curves of the optimized PSCs based on the four polymers as donors and Y6 as acceptors with a donor/acceptor weight ratio of 1:1.2, and **Table 1** lists the photovoltaic performance parameters of the corresponding devices. It can be seen from Table 1 that the devices based on polymers PTQ7, PTQ9, and PTQ10 exhibit gradually increasing V_{oc} of 0.71, 0.82, and 0.87 V with increasing the number of F atoms substitution on Qx A-unit, which are consistent with the downshifted E_{HOMO} of the polymer donors. The PCE of the PSCs based on polymers PTQ7, PTQ9, and PTQ10 gradually increased from 5.75% for PTQ7 to 10.50% for PTQ9 and to 16.21% for PTQ10 with simultaneously enhanced J_{sc} and FF. However, the device based on polymer PTQ8 shows extremely low J_{sc} and FF, resulting in the lowest PCE of 0.90% though it has the highest V_{oc}, which should be ascribed to the mismatched E_{HOMO} between polymer PTQ8 and acceptor Y6 (the E_{HOMO} of the donor PTQ8 is lower than that of the acceptor Y6), thus causing the poor exciton dissociation and charge transport in the blend film.

To confirm photovoltaic performance of the PSCs based on the four polymers, we measured the external quantum efficiency (EQE) of the corresponding champion devices, and the results are shown in Figure 2b. In comparison with the PTQ7-based device, the devices based on polymers PTQ9 and PTQ10 show enhanced photoelectric conversion efficiency with comprehensively rising EQE profiles (maximal EQE value of 79.08% for the PTQ9-based device and 80.8% for the PTQ10-based device, compared to 61.89% for the PTQ7-based device). The current density values integrated from the EQE spectra are 18.09 mA cm^{-2} for the PTQ7-based device, 23.07 mA cm^{-2} for the PTQ9-based device, and 23.76 mA cm^{-2} for the PTQ10-based device, which are consistent well with the J_{sc} values from *J–V* curves within 5% mismatch, indicating the reliability of the measured photovoltaic data. Consistent with the result from *J–V* measurement, the PTQ8-based device shows an extremely poor photoelectric response with a maximal EQE value of ≈10% and a low integrated current density of 3.05 mA cm^{-2}, which should be ascribed to the poor charge separation in the blend due to the HOMO energy level mismatching.

Table 1. Photovoltaic performance parameters of the PSCs based on polymer:Y6.

Devices	V_{oc} [V]	J_{sc} [mA cm^{-2}]	FF [%]	PCE [%]
PTQ7:Y6	0.71	18.65	43.4	5.75 (5.69 ± 0.06)[a]
PTQ8:Y6	0.89	3.11	32.5	0.90 (0.86 ± 0.02)
PTQ9:Y6	0.82	23.72	54.0	10.50 (10.30 ± 0.13)
PTQ10:Y6	0.87	24.81	75.1	16.21 (15.97 ± 0.18)

[a]The average values are calculated from 20 devices.

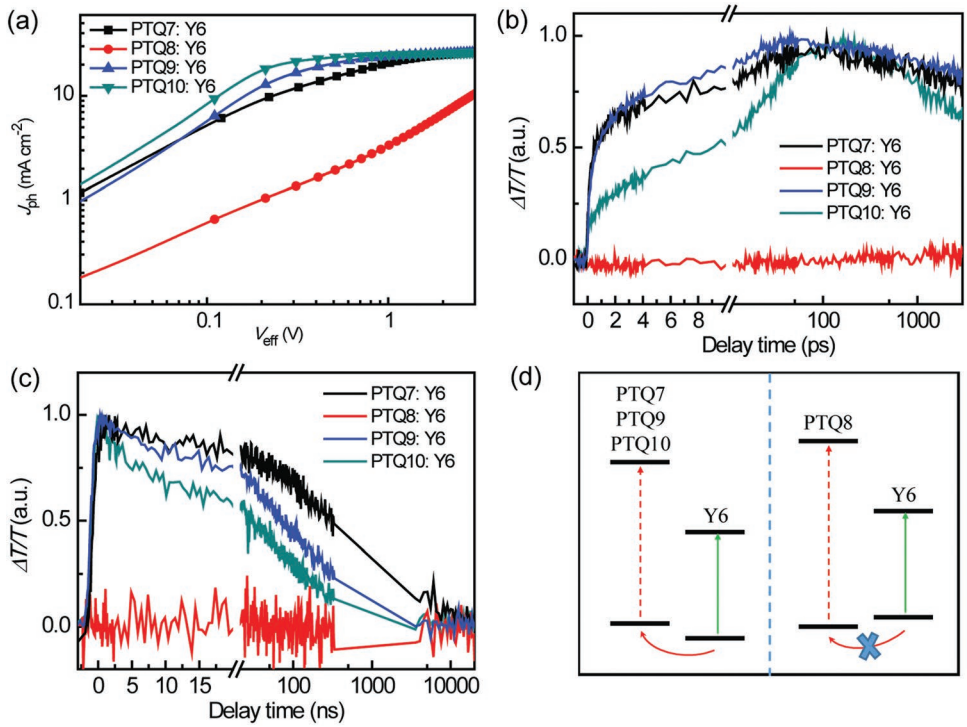

Figure 3. a) J_{ph} versus V_{eff} of the PSCs based on polymer:Y6. b) The femtosecond-resolved (excited by 800 nm) and c) nanosecond-resolved (excited by 532 nm) TA dynamic curves probed at 620 nm from PTQ7:Y6 blend, 570 nm from PTQ8:Y6 blend, 630 nm from PTQ9:Y6 blend, and 615 nm from PTQ10:Y6 blend, respectively. d) A schematic diagram of the hole transfers in the polymer:Y6 blends.

Charge separation and transport are the crucial processes from photons to electrons conversion in the PSCs. As mentioned above, fluorination results in the downshifted E_{HOMO} of polymers PTQ8, PTQ9, and PTQ10, and the gradually smaller E_{HOMO} offset ($\Delta E_{HOMO(D-A)}$) between polymer donors and acceptors ($\Delta E_{HOMO(D-A)}$ becomes negative for the PTQ8:Y6 blend). In order to investigate the effect of the E_{HOMO} offset on the exciton dissociation dynamics of the devices, we studied the relationship between the photocurrent density (J_{ph}) and the effective voltage (V_{eff}).[33] As expected, the PTQ8-based device exhibits an extremely low exciton dissociation probability of 46.6% (see **Figure 3**a), which should be caused by the mismatched E_{HOMO} alignment between donor PTQ8 and acceptor Y6. In contrast, the devices based on the polymers PTQ9 and PTQ10 with monofluoro-substituted and difluoro-substituted Qx A-unit show gradually increased exciton dissociation probability of 92.6% and 96.2% (75.3% for PTQ7-based device), respectively.

To further study the effect of fluorination forms on the photoinduced charge-separation and charge-transfer dynamics in the devices based on the four polymers,[34] we performed the TA spectroscopy measurements (the detailed measurement method is described in the Supporting Information) to check the charge-transfer details. As all of the four polymer:Y6 combinations possess sufficient $\Delta E_{LUMO(D-A)}$ (>1 eV) for electron transfer, thus, here we mainly focused on the hole-transfer process in the four blends. We performed the femtosecond-resolved TA spectroscopy measurements to probe the hole-transfer process in the blends at the excitation wavelength of 800 nm, and only acceptor Y6 was excited at this pump wavelength according to the TA signals from the neat samples of polymers (Figure S2, Supporting Information). The corresponding TA results of the blends based on the four polymers are shown in Figure 3b and Figure S3 (Supporting Information). It is found that there were no bleaching signals observed in the PTQ8-based blend, which indicates that there is almost no hole transfer in the blend. This result is consistent with the exciton dissociation measurements mentioned above, which should be due to the mismatched E_{HOMO} alignment between donor PTQ8 and acceptor Y6. In contrast, the obvious bleaching signals at the shorter-wavelength range were observed from the blends based on PTQ7, PTQ9, and PTQ10 though the gradually reduced $\Delta E_{HOMO(D-A)}$. As the excitation photon energy at 800 nm is much smaller than that required for exciton absorption of polymers, therefore, those bleaching signals can be naturally assigned to the efficient hole transfer from Y6 to polymers. Moreover, all the three blends exhibit long enough charge separated (CS) state lifetimes with nanosecond scale from the nanosecond-resolved TA spectroscopy (Figure 3c; Figure S4, Supporting Information). With these results, we briefly summarize that fast and efficient hole transfer is achieved in the blends based on PTQ7, PTQ9, and PTQ10 (Figure 3d), and it suggests the existence of the long-lived dissociated excitons in the blends, which is beneficial for electricity generation. In contrast, the PTQ8-based blend shows extremely poor charge-separation and hole-transfer behaviors due to the mismatched E_{HOMO} alignment (negative $\Delta E_{HOMO(D-A)}$) between donor PTQ8 and acceptor Y6.

The V_{loss} in solar cells is defined as the difference between the E_g/q (q is the elementary charge) of the solar cells' active layer (for the PSCs, the lowest E_g value between the donor

Table 2. Detailed V_{loss} parameters of the PSCs based on polymer:Y6.

Devices	E_g [eV]	V_{OC}^{SQ} [V]	ΔE_1 [eV]	V_{OC}^{rad} [V]	ΔE_2 [eV]	ΔE_3 [eV]	V_{loss} [V]
PTQ7:Y6	1.414	1.16	0.254	1.06	0.10	0.35	0.704
PTQ9:Y6	1.422	1.16	0.262	1.07	0.09	0.25	0.602
PTQ10:Y6	1.419	1.16	0.259	1.10	0.06	0.23	0.549

and acceptor is used in the calculation) and its V_{oc}. In order to investigate the intrinsic reasons that cause the dramatically changed V_{oc}, V_{loss}, and photovoltaic performance of the devices, here we systematically studied the V_{loss} issue of the PSCs based on the polymer donors of PTQ7, PTQ9, and PTQ10 (we will not discuss the V_{loss} of the PTQ8-based device due to its mismatched HOMO energy level with acceptor Y6). The detailed components of V_{loss} can be categorized into three parts based on the SQ limit, as shown in Equation (1)[29]

$$\begin{aligned} qV_{loss} &= E_g - qV_{OC} \\ &= \left(E_g - qV_{OC}^{SQ}\right) + \left(qV_{OC}^{SQ} - qV_{OC}^{rad}\right) + \left(qV_{OC}^{rad} - qV_{OC}\right) \\ &= \left(E_g - qV_{OC}^{SQ}\right) + q\Delta V_{OC}^{rad,\,below\ gap} + q\Delta V_{OC}^{non\text{-}rad} \\ &= \Delta E_1 + \Delta E_2 + \Delta E_3 \end{aligned} \tag{1}$$

$$\Delta E_1 = E_g - qV_{OC}^{SQ} \cong E_g - \frac{kT}{q}\ln\left\{\frac{q\cdot\int_{E_g}^{+\infty}\varnothing_{AM1.5G}(E)\cdot dE}{q\cdot\int_{E_g}^{+\infty}\varnothing_{BB}(E)\cdot dE}\right\} \tag{2}$$

The first two parts (ΔE_1 and ΔE_2) in Equation (1) are caused by radiative recombination, and the third part (ΔE_3) is caused by nonradiative recombination. The ΔE_1 is the unavoidable loss for all types of solar cells, which is from the mismatch between received radiative in a narrow solid angle from sun and the omnidirectional radiative recombination. The value of ΔE_1 is only determined by E_g for a given illumination spectrum and temperature according to Equation (2). As all of the four devices using the same acceptor Y6, thus the values of ΔE_1 were calculated to be nearly identical (**Table 2**; Figure S5, Supporting Information, the calculation of ΔE_1, ΔE_2, and ΔE_3 is described in the Supporting Information). The minor difference of ΔE_1 is due to the slight difference in molecular packing behavior of acceptor Y6 when blending with different polymer donors

$$\begin{aligned} \Delta E_2 &= qV_{OC}^{SQ} - qV_{OC}^{rad} \\ &\cong \frac{kT}{q}\left[\ln\left\{\frac{q\cdot\int_{E_g}^{+\infty}\varnothing_{AM1.5G}(E)\cdot dE}{q\cdot\int_{E_g}^{+\infty}\varnothing_{BB}(E)\cdot dE}\right\} - \ln\left\{\frac{q\cdot\int_{0}^{+\infty}EQE(E)\cdot\varnothing_{AM1.5G}(E)\cdot dE}{q\cdot\int_{0}^{+\infty}EQE(E)\cdot\varnothing_{BB}(E)\cdot dE}\right\}\right] \end{aligned} \tag{3}$$

The ΔE_2 is the additional radiative recombination loss from the absorption below the bandgap which is attributed to the non-step function absorption or EQE in the realistic PSCs devices. To probe the V_{loss} from this part, we carried out the Fourier-transform photocurrent spectroscopy (FTPS; the detailed measurement method is described in the Supporting Information) and EL measurements (**Figure 4**a) of the three devices. The values of ΔE_2 were calculated to be 0.06–0.10 eV according to Equation (3) (Table 2); the small ΔE_2 values mean the radiative recombination loss from the absorption below the bandgap is insignificant and it only contributes to a small part of V_{loss} for the three devices

$$\Delta E_3 = qV_{OC}^{rad} - qV_{OC} = q\Delta V_{OC}^{non\text{-}rad} \tag{4}$$

The third part ΔE_3 is the loss from nonradiative recombination in the devices (Equation (4)). For inorganic solar cells and pero-SCs, ΔE_3 is about 0.25 eV, while this value is much larger

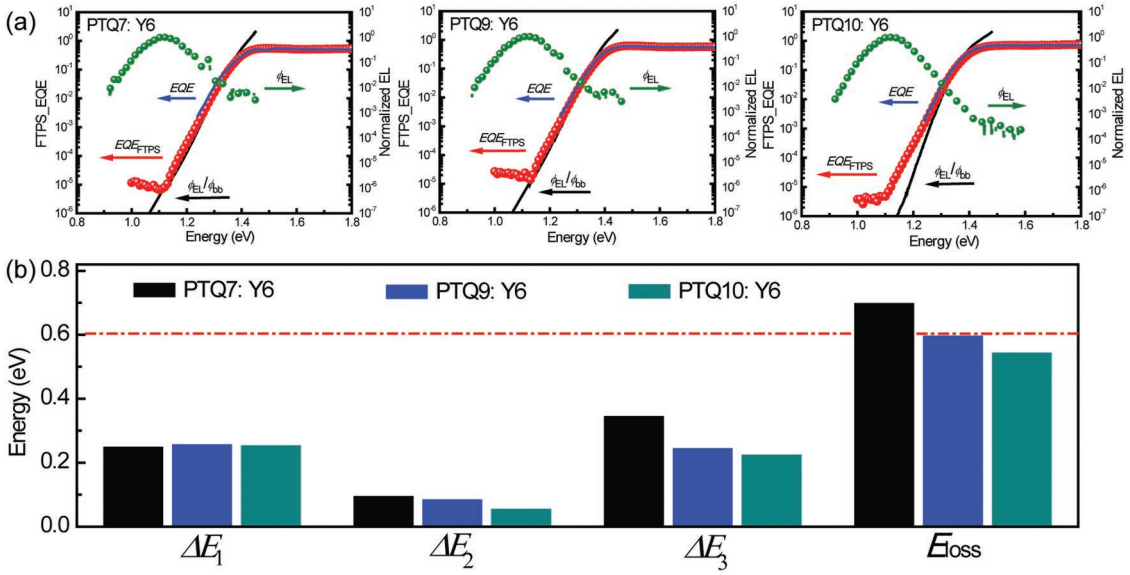

Figure 4. a) FTPS–EQE, EQE, normalized EL, and ϕ_{EL}/ϕ_{bb} of the devices based on polymer:Y6. b) E_{loss} and its detailed three components of ΔE_1, ΔE_2, and ΔE_3.

in PSCs (generally in the range of 0.38–0.44 eV). To study the effect of fluorination forms on the nonradiative recombination loss, we estimate the V_{OC}^{rad} values of the three devices by the FTPS and EL measurements, and they were calculated to be 1.06 V for the PTQ7-based device, 1.07 V for the PTQ9-based device, and 1.10 V for the PTQ10-based device; thus, the corresponding ΔE_3 values were 0.35, 0.25, and 0.23 eV respectively (Table 2). It is found that the devices based on the fluorinated polymers PTQ9 and PTQ10 show obviously reduced ΔE_3 in comparison with the PTQ7-based device, and the values of ΔE_3 gradually decrease as the degree of fluorination on Qx A-unit increases.

Figure 4b displays the energy loss (E_{loss}) and its detailed three components. It is found that unavoidable radiative recombination loss ΔE_1 and nonradiative recombination loss ΔE_3 constitute the main part of E_{loss}, and the difference of E_{loss} is mainly caused by the ΔE_3. As increasing the number of F atom substitutions on the Qx A-unit of the polymer donors, the corresponding devices show gradually reduced E_{loss}. As a result, the PTQ10-based device demonstrates an impressive PCE of 16.21% with an extremely low V_{loss} of 0.549 V which is one of the lowest V_{loss} values in the highly efficient PSCs. The results indicate that rational fluorination of the polymer donors is an effective method to suppress nonradiative recombination loss thus reducing V_{loss} of the PSCs.

Morphology of the photoactive layer is a critical factor to determine the donor/acceptor blend quality and the photovoltaic performance of the PSCs. To probe the fluorination effects on molecular self-assembly, molecular orientation features, and blend films' morphology, we carried out grazing-incidence wide-angle X-ray diffraction (GIWAXS) measurements, and the images and plots of GIWAXS measurements are shown in **Figure 5**. For the neat PTQ7 film, there is no π–π stacking diffraction peaks ((010) peaks) in both of in-plane (IP) and out-of-plane (OOP) directions (Figure 5a,c), which indicates the amorphous feature of the polymer PTQ7. For the neat PTQ9 and PTQ10 films with monofluoro-substituted and difluoro-substituted Qx A-units, the distinct and gradually enhanced (010) peaks were observed at 1.71 and 1.73 $Å^{-1}$ in OOP directions (Figure 5a,c) which correspond to the reduced π–π stacking distance of 3.67 and 3.63 Å, respectively, and a gradually decreased lamellar distance was also observed in the neat PTQ9 (23.28 Å) and PTQ10 (23.27 Å) films in comparison with 25.54 Å for neat PTQ7 film. The gradually increased (010) peaks, reduced π–π stacking distance and reduced lamellar distance in the OOP directions of the polymers PTQ9 and PTQ10 suggest more preference of face-on molecular packing orientation in the vertical direction of substrate, which are beneficial for efficient charge transport in the films. For the neat acceptor Y6 film, the obvious face-on molecular packing orientation with π–π stacking diffraction peaks at ≈1.7 $Å^{-1}$ in the OOP direction is observed (Figure S6, Supporting Information). The GIWAXS plots of blend films demonstrate microstructural features with the diffraction patterns contributed from individual components (Figure 5b,d). In comparison with the PTQ7-based blend film, just like the molecular stacking features of the neat PTQ9 and PTQ10 films, the PTQ9-based and PTQ10-based blends exhibit more preferred face-on molecular packing orientation and more tight molecular packing features in the OOP direction, indicating the better charge transport capability in the vertical direction of substrate. The results indicate that fluorination on the Qx A-unit of the PTQ derivative donors results in partial aggregation of the polymer chains thus leading to the enhanced π–π molecular stacking features and the higher molecular crystalline characteristics of polymers PTQ9 and PTQ10, which consequently assist charge transport and improve the photovoltaic performance of the PSCs based on PTQ9 and PTQ10. The gradually increased molecular self-assembly features of polymers PTQ9 and PTQ10 and the more favorable morphology of their blend films can also be observed from the topography images of their blend films (Figure S7, Supporting Information).

The hole mobilities (μ_h) of the PSCs based on PTQ7, PTQ9, and PTQ10 as donors are measured using the space charge limited current (SCLC) method with the hole-only devices (ITO/PEDOT:PSS/polymer:Y6/Au), and the measurement results are shown in Figure S8 (Supporting Information). As expected, the device based on polymer PTQ7 without fluorine substitution shows the lowest μ_h of 0.48×10^{-5} cm^2 V^{-1} s^{-1}; the poor hole transport capability will cause serious recombination behavior in the blend thus resulting in low J_{sc}, FF, and poor photovoltaic performance. The PTQ9-based and PTQ10-based devices show gradually increased μ_h of 1.20×10^{-5} and 3.12×10^{-5} cm^2 V^{-1} s^{-1}, respectively, in comparison with the PTQ7-based device. The improved hole mobility suggests better hole transport capability of the fluorinated polymers PTQ9 and PTQ10, which could be responsible for the increased J_{sc} and FF of the PTQ9-based and PTQ10-based PSCs.

The charge-carrier recombination behavior of the three PSCs based on PTQ7:Y6, PTQ9:Y6, and PTQ10:Y6 is investigated according to the dependence of J_{sc} and V_{oc} on light intensity (P_{light}), respectively. In PSCs, J_{sc} and P_{light} follow the relationship of $J_{sc} \propto (P_{light})^{\alpha}$, where the α value indicates the degree of bimolecular recombination. If all free charge carriers are collected prior to recombination, the α value should be 1, while $\alpha < 1$ indicates there is some extent of bimolecular recombination. Figure S9a (Supporting Information) shows the plots of log J_{sc} versus log P_{light}, and the slope α values are 0.92 for the PTQ7:Y6-based device, 0.98 for the PTQ9:Y6-based device, and 0.99 for the PTQ10:Y6-based device. The α values gradually approach 1 for the PTQ9:Y6-based device and PTQ10:Y6-based device indicate the gradually reduced bimolecular recombination and more efficient charge carrier transportation feature in their blends. In addition, if bimolecular recombination is the exclusive recombination forms in PSCs, the slope of the fitting straight line of V_{oc} versus ln (P_{light}) should be kT/q (where q is the elementary charge, k is the Boltzmann constant, and T is the Kelvin temperature), the plots of V_{oc} versus ln (P_{light}) of the three devices are shown in Figure S9b (Supporting Information). The slopes of the fitting lines for the PSCs based on PTQ7:Y6, PTQ9:Y6, and PTQ10:Y6 are 1.32, 1.23, and 1.02 kT/q, respectively. The slope very close to kT/q for the PTQ10:Y6-based device indicates that there are very few other recombination forms in its blend. The results of J_{sc} and V_{oc} dependence on P_{light} indicate that there is very few charge-carrier recombination in the PTQ10:Y6-based PSC. Typically, charge-carrier recombination is directly related to FF of the PSCs. This result together with the higher hole mobility of PTQ10:Y6 blend should be contributed to the higher FF value (75.1%) of the PSC based on PTQ10:Y6.

In conclusion, we develop four low-cost D–A copolymer donors of PTQ derivatives based on electron-rich thiophene D-unit and electron-deficient Qx A-unit with different fluorine substituents, to investigate the effect of fluorination forms on charge-separation behaviors and V_{loss} of the

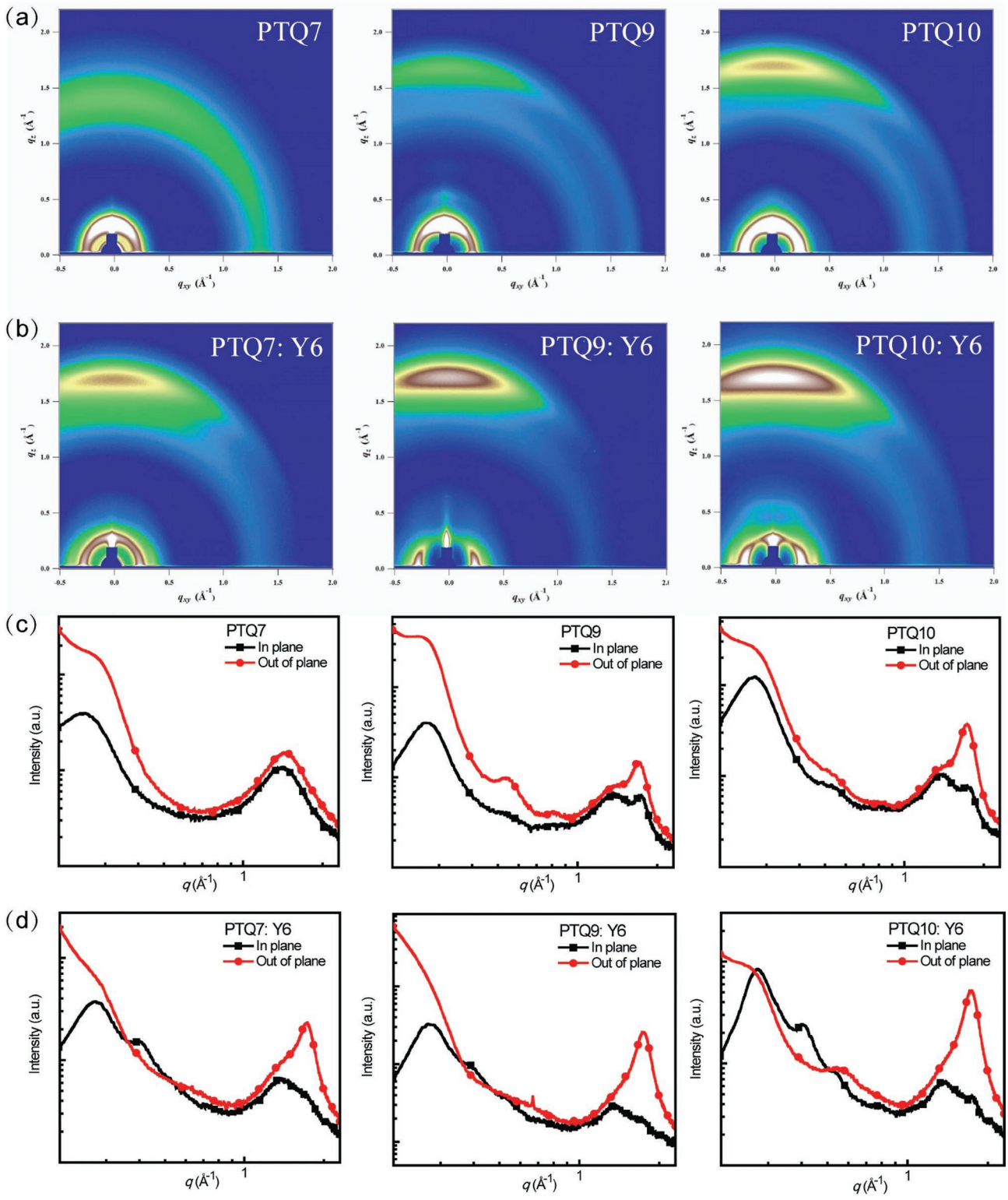

Figure 5. a) GIWAXS images and c) line cuts of the neat PTQ7 film, neat PTQ9 film, and neat PTQ10 film. b) GIWAXS images and d) line cuts of the PTQ7:Y6 blend film, PTQ9:Y6 blend film, and PTQ10:Y6 blend film.

PTQ-derivative-based PSCs. In comparison with PTQ7 without fluorination, the fluorination on other three polymers results in downshifted E_{HOMO}, especially PTQ8 with bifluorine substitution on thiophene D-unit shows the lowest E_{HOMO} of –5.68 eV. The PTQ8-based device displays a highest V_{oc} of 0.89 V but very poor PCE of 0.90% with the low J_{sc} and low FF because of the

extremely poor charge separation and transportation in the blend resulting from the mismatched E_{HOMO} alignment between donor PTQ8 and acceptor Y6. While PTQ9 and PTQ10 with fluorination on their Qx A-unit possess lower and appropriate E_{HOMO}, and the PSCs with PTQ9 and PTQ10 as donors exhibit higher PCE with higher V_{oc} (lower V_{loss}), higher J_{sc} and higher FF simultaneously, in comparison with the PTQ7-based device. Moreover, the two devices show gradually enhanced charge separation and transport behavior with increasing number of F atoms on Qx A-unit from photocurrent measurement and the TA spectra. Importantly, the PTQ10-based device with Y6 as acceptors demonstrates an impressive PCE of 16.21% with a high V_{oc} of 0.87 V (low V_{loss} of 0.549 V) and a large J_{sc} of 24.81 mA cm^{-2} simultaneously, and a V_{loss} of 0.549 V is one of the lowest V_{loss} values in the efficient PSCs with PCE over 15%. The results indicate that rational fluorination of the polymer donors is the effective method to achieve fast charge separation and low V_{loss} simultaneously in the PSCs, which is beneficial for obtaining the highly efficient PSCs with both high V_{oc} and large J_{sc}.

Supporting Information

Supporting Information is available from the Wiley Online Library or from the author.

Acknowledgements

C.S. and F.P. contributed equally to this work. This work was supported by National Natural Science Foundation of China (Grant Nos. 91633301, 21734008, and 51820105003) and the Strategic Priority Research Program of the Chinese Academy of Sciences (Grant No. XDB12030200).

Conflict of Interest

The authors declare no conflict of interest.

Keywords

charge separation, fluorination, low-cost copolymer donors, nonradiative recombination, voltage loss

Received: August 23, 2019
Revised: October 17, 2019
Published online: November 14, 2019

[1] G. Yu, J. Gao, J. C. Hummelen, F. Wudl, A. J. Heeger, *Science* **1995**, *270*, 1789.
[2] C. Li, M. Liu, N. G. Pschirer, M. Baumgarten, K. Mullen, *Chem. Rev.* **2010**, *110*, 6817.
[3] Y. Kim, S. Cook, S. M. Tuladhar, S. A. Choulis, J. Nelson, J. R. Durrant, D. D. C. Bradley, M. Giles, I. McCulloch, C.-S. Ha, M. Ree, *Nat. Mater.* **2006**, *5*, 197.
[4] L. Huo, S. Zhang, X. Guo, F. Xu, Y. Li, J. Hou, *Angew. Chem., Int. Ed.* **2011**, *50*, 9697.
[5] J. Zhao, Y. Li, G. Yang, K. Jiang, H. Lin, H. Ade, W. Ma, H. Yan, *Nat. Energy* **2016**, *1*, 15027.
[6] H. Bin, L. Gao, Z.-G. Zhang, Y. Yang, Y. Zhang, C. Zhang, S. Chen, L. Xue, C. Yang, M. Xiao, Y. F. Li, *Nat. Commun.* **2016**, *7*, 13651.
[7] C. Sun, F. Pan, H. Bin, J. Zhang, L. Xue, B. Qiu, Z. Wei, Z.-G. Zhang, Y. F. Li, *Nat. Commun.* **2018**, *9*, 743.
[8] Y. He, H.-Y. Chen, J. Hou, Y. F. Li, *J. Am. Chem. Soc.* **2010**, *132*, 1377.
[9] Y. Lin, J. Wang, Z.-Z. Zhang, H. Bai, Y. F. Li, D. Zhu, X. Zhan, *Adv. Mater.* **2015**, *27*, 1170.
[10] Q. Fan, W. Su, Y. Wang, B. Guo, Y. Jiang, X. Guo, F. Liu, T. P. Russell, M. Zhang, Y. F. Li, *Sci. China: Chem.* **2018**, *61*, 531.
[11] J. Yuan, Y. Zhang, L. Zhou, G. Zhang, H.-L. Yip, T.-K. Lau, X. Lu, C. Zhu, H. Peng, P. A. Johnson, M. Leclerc, Y. Cao, J. Ulanski, Y. F. Li, Y. Zou, *Joule* **2019**, *3*, 1140.
[12] C. J. Brabec, S. E. Shaheen, C. Winder, N. S. Sariciftci, P. Denk, *Appl. Phys. Lett.* **2002**, *80*, 1288.
[13] J. Y. Kim, S. H. Kim, H.-H. Lee, K. Lee, W. Ma, X. Gong, A. J. Heeger, *Adv. Mater.* **2006**, *18*, 572.
[14] Z. He, C. Zhong, X. Huang, W.-Y. Wong, H. Wu, L. Chen, S. Su, Y. Cao, *Adv. Mater.* **2011**, *23*, 4636.
[15] Z. A. Page, Y. Liu, V. V. Duzhko, T. P. Russell, T. Emrick, *Science* **2014**,*346*, 441.
[16] Z.-G. Zhang, B. Qi, Z. Jin, D. Chi, Z. Qi, Y. F. Li, J. Wang, *Energy Environ. Sci.* **2014**, *7*, 1966.
[17] G. Li, V. Shrotriya, J. Huang, Y. Yao, T. Moriarty, K. Emery, Y. Yang, *Nat. Mater.* **2005**, *4*, 864.
[18] M. Campoy-Quiles, T. Ferenczi, T. Agostinelli, P. G. Etchegoin, Y. Kim, T. D. Anthopoulos, P. N. Stavrinou, D. D. C. Bradley, J. Nelson, *Nat. Mater.* **2008**, *7*, 158.
[19] L. Ye, S. Zhang, W. Ma, B. Fan, X. Guo, Y. Huang, H. Ade, J. Hou, *Adv. Mater.* **2012**, *24*, 6335.
[20] X. Xu, K. Feng, Z. Bi, W. Ma, G. Zhang, Q. Peng, *Adv. Mater.* **2019**, *31*, 1901872.
[21] Y. Cui, H. Yao, J. Zhang, T. Zhang, Y. Wang, L. Hong, K. Xian, B. Xu, S. Zhang, J. Peng, Z. Wei, F. Gao, J. Hou, *Nat. Commun.* **2019**, *10*, 2515.
[22] J. Liu, S. Chen, D. Qian, B. Gautam, G. Yang, J. Zhao, J. Bergqvist, F. Zhang, W. Ma, H. Ade, O. Inganäs, K. Gundogdu, F. Gao, H. Yan, *Nat. Energy* **2016**, *1*, 16089.
[23] J. Yao, T. Kirchartz, M. S. Vezie, M. A. Faist, W. Gong, Z. He, H. Wu, J. Troughton, T. Watson, D. Bryant, J. Nelson, *Phys. Rev. Appl.* **2015**, *4*, 014020.
[24] M. T. Dang, L. Hirsch, G. Wantz, *Adv. Mater.* **2011**, *23*, 3597.
[25] T. Linderl, T. Zechel, M. Brendel, D. M. González, P. Müller-Buschbaum, J. Pflaum, W. Brütting, *Adv. Energy Mater.* **2017**, *7*, 1700237.
[26] Y. Wang, D. Qian, Y. Cui, H. Zhang, J. Hou, K. Vandewal, T. Kirchartz, F. Gao, *Adv. Energy Mater.* **2018**, *8*, 1801352.
[27] J. Yuan, T. Huang, P. Cheng, Y. Zou, H. Zhang, J. L. Yang, S.-Y. Chang, Z. Zhang, W. Huang, R. Wang, D. Meng, F. Gao, Y. Yang, *Nat. Commun.* **2019**, *10*, 570.
[28] K. Vandewal, K. Tvingstedt, A. Gadisa, O. Inganäs, J. V. Manca, *Nat. Mater.* **2009**, *8*, 904.
[29] S. Chen, Y. Wang, L. Zhang, J. Zhao, Y. Chen, D. Zhu, H. Yao, G. Zhang, W. Ma, R. H. Friend, P. C. Y. Chow, F. Gao, H. Yan, *Adv. Mater.* **2018**, *30*, 1804215.
[30] Y. Xie, T. Li, J. Guo, P. Bi, X. Xue, H. S. Ryu, Y. Cai, J. Min, L. Huo, X. Hao, H. Y. Woo, X. Zhan, Y. Sun, *ACS Energy Lett.* **2019**, *4*, 1196.
[31] X. Li, F. Pan, C. Sun, M. Zhang, Z. Wang, J. Du, J. Wang, M. Xiao, L. Xue, Z.-G. Zhang, C. Zhang, F. Liu, Y. F. Li, *Nat. Commun.* **2019**, *10*, 519.
[32] R. Xue, J. Zhang, Y. Li, Y. F. Li, *Small* **2018**, *14*, 1801793.
[33] H. Bin, J. Yao, Y. Yang, I. Angunawela, C. Sun, L. Gao, L. Ye, B. Qiu, L. Xue, C. Zhu, C. Yang, Z.-G. Zhang, H. Ade, Y. F. Li, *Adv. Mater.* **2018**, *30*, 1706361.
[34] A. Timalsina, P. E. Hartnett, F. S. Melkonyan, J. Strzalka, V. S. Reddy, A. Facchetti, M. R. Wasielewski, T. J. Marks, *J. Mater. Chem. A* **2017**, *5*, 5351.

